Cerebral Cortex February 2011;21:392–400
doi:10.1093/cercor/bhq106
Advance Access publication June 10, 2010

Cognitive Decline Is Associated with Reduced Reelin Expression in the Entorhinal Cortex of Aged Rats

Alexis M. Stranahan, Rebecca P. Haberman and Michela Gallagher

Department of Psychological and Brain Sciences, Johns Hopkins University, Baltimore, MD 21218, USA

Address correspondence to Michela Gallagher, PhD, Department of Psychological and Brain Sciences, Johns Hopkins University, 3400 North Charles Street, Baltimore, MD 21218, USA. Email: michela@jhu.edu.

Brain regions and neural circuits differ in their vulnerability to changes that occur during aging and in age-related neurodegenerative diseases. Among the areas that comprise the medial temporal lobe memory system, the layer II neurons of the entorhinal cortex, which form the perforant path input to the hippocampal formation, exhibit early alterations over the course of aging Reelin, a glycoprotein implicated in synaptic plasticity, is expressed by entorhinal cortical layer II neurons. Here, we report that an age-related reduction in reelin expression in the entorhinal cortex is associated with cognitive decline. Using immunohistochemistry and in situ hybridization, we observed decreases in the number of Reelin-immunoreactive cells and reelin messenger RNA expression in the lateral entorhinal cortex of aged rats that are cognitively impaired relative to young adults and aged rats with preserved cognitive abilities. The lateral entorhinal cortex of aged rats with cognitive impairment also exhibited changes in other molecular markers, including increased accumulation of phosphorylated tau and decreased synaptophysin immunoreactivity. Taken together, these findings suggest that reduced reelin expression, emanating from layer II entorhinal neurons, may contribute to network dysfunction that occurs during memory loss in aging.

Keywords: aging, Alzheimer's disease, lateral entorhinal cortex, learning, mild cognitive impairment

Cognitive deficits that commonly occur during aging are associated with the disruption of specific neural networks. The layer II neurons in the entorhinal cortex, which form a key circuit in the medial temporal lobe memory system, have a particular vulnerability that extends across a spectrum of age-related memory loss, including amnestic mild cognitive impairment (MCI) and Alzheimer's disease (AD). These neurons are functionally positioned at the intersection of information processing in cortical networks and the hippocampal formation, and they provide the majority of input to the dentate gyrus and CA3 areas of the hippocampus (van Strien et al. 2009). The reasons for their selective vulnerability to aging and AD, however, remain unclear.

In rodent models of aging, entorhinal cortical neurons are not lost (Merrill et al. 2001; Rapp et al. 2002), but synaptic connections are reduced in the terminal zones that are densely innervated by layer II afferents (Geinisman et al. 1978; Smith et al. 2000). Loss of innervation occurs only in aged rats with hippocampal-dependent memory impairment, whereas rats that age without cognitive decline have preserved entorhinal connections (Smith et al. 2000). A similar topographical vulnerability occurs in humans, such that entorhinal innervation of the dentate gyrus declines as a function of worsening memory performance in normal aging, MCI and AD (Scheff et al. 2006). Frank loss of entorhinal layer II neurons is apparent in mild AD, further disconnecting cortical processing from the hippocampal formation (Gómez-Isla et al. 1996). Because the cellular basis for entorhinal layer II vulnerability remains undetermined in these conditions, it is of interest to identify specific molecular features of those neurons in cognitive aging, which may give clues about the earliest changes associated with hippocampal network dysfunction.

Reelin is a large glycoprotein with widespread expression in interneurons throughout the brain. Certain populations of excitatory neurons also express reelin, and entorhinal layer II neurons are among this group (Ramos-Moreno et al. 2006). Reelin signaling negatively regulates tau phosphorylation (Hiesberger et al. 1999); conversely, reelin depletion creates a permissive environment for cellular events that are tied to the pathophysiology of AD (Hiesberger et al. 1999; Hoe et al. 2009). Reductions in reelin expression have been reported in the entorhinal cortex of mouse models of AD and in the human AD brain (Chin et al. 2007), but it remains to be determined whether this is a condition specific to AD pathology. No studies have addressed the possibility that changes in entorhinal cortical reelin levels might be related to cognitive function over the course of normal aging.

Individual differences in cognitive aging exist in humans and in rodent populations. We used a well-characterized model in which aged rats are classified based on the presence or absence of memory impairments, with associated functional alterations in the medial temporal lobe (Gallagher and Rapp 1997; Wilson et al. 2006). Here, we report that reelin expression in the lateral entorhinal cortex is reduced in aged rats with memory impairment. This was observed in a stereological analysis and in an assessment of reelin messenger RNA (mRNA) by in situ hybridization. In both studies, changes in aged rats with memory impairment clearly affected the lateral but not the medial entorhinal cortex. Reelin depletion occurred in conjunction with significant increases in tau phosphorylation affecting the lateral entorhinal region, possibly recapitulating the localization of early tangle formation in human aging and AD (Braak H and Braak E 1995). The lateral entorhinal cortex also exhibits a loss of synaptic marker expression with age-related cognitive impairment. These signatures in rats with memory impairment represent a change in aging that could contribute to the selective vulnerability of entorhinal cortical neurons and to reduced integrity of the perforant path circuit innervating the hippocampal formation.

Materials and Methods

Animals and Behavioral Characterization

Male Long-Evans rats, obtained from Charles River Laboratories, were 6 (adult) or 24 (aged) months of age at the time of the studies. All rats were individually housed for 2 months to acclimate to the vivarium

before behavioral testing, which took place as described (Boric et al. 2008). Training occurred over 8 days in sessions of 3 trials per day with a 60-s intertrial interval. During the trials, rats were placed in the water at the perimeter of the pool, with starting locations varied across trials. Each trial lasted for 90 s or until the rat successfully located the platform. Every sixth trial was a probe trial to assess the rat's spatial bias during its search. Rats were permitted to escape on probe trials when a retracted platform was made available after 30 s for completion of those trials. An index score, derived from the proximity of the rat to the escape platform location during the 30-s free swim on probe trials, was used to characterize performance of the rats in the maze for the purpose of neurobiological analyses. This index is the sum of the weighted proximity scores measured during the probe trials, with lower scores reflecting better spatial memory as indicated by shorter average distances from the platform location (Gallagher et al. 1993). For immunohistochemistry experiments, we analyzed tissue from (n = 9) young, (n = 9) aged-impaired, and (n = 9) aged-unimpaired rats. For in situ hybridization, we used tissue from (n = 5) young, (n = 6) aged-impaired, and (n = 6) aged-unimpaired rats.

Euthanasia and Tissue Preparation

For immunohistochemistry, rats were anesthetized with isoflurane and perfused transcardially with sterile saline, followed by 4% paraformaldehyde in phosphate buffer. After 24 h postfixation, brains were moved into progressively increasing concentrations of glycerol in phosphate buffer. Brains were then sectioned on the coronal plane in a 1 in 10 series at 50 μm thickness. Sections were stored in cryoprotectant at −80 °C.

For in situ hybridization, rats were anesthetized, perfused, and brains were postfixed as described above. After postfixation, brains were moved into 4% paraformaldehyde in phosphate buffer containing 20% sucrose for dehydration and cryoprotection. Brains were then frozen on dry ice and stored at −80 °C prior to sectioning. A 1 in 12 series of coronal sections (30 μm) were cut using a freezing microtome and stored in 4% paraformaldehyde at 4 °C.

Immunohistochemistry and Immunofluorescence

For reelin peroxidase labeling, free-floating sections were incubated in 3.0% H_2O_2 in phosphate-buffered saline (PBS) to quench endogenous peroxidases. Sections were rinsed, then reacted in 0.1 M citric acid for 10 min. After additional rinses, the tissue was moved into primary antibody solution containing mouse anti-reelin (1:1000, Chemicon) with 0.25% Tween-20. The tissue was reacted in primary antibody solution at 4 °C for 48 h with shaking. After primary antibody incubation, tissue sections were rinsed in PBS, then blocked in 5% horse serum in PBS containing 0.25% Tween-20. Primary antibodies were then detected with biotin-labeled secondary horse anti-mouse and amplified with avidin–biotin complex (Vector Labs). Diaminobenzadine was used as a chromogen.

For reelin/synaptophysin double labeling, tissue was treated with 1.5% sodium borohydride in tris-buffered saline (TBS) for 30 min to reduce autofluorescence. Sections were then reacted with primary antibodies mouse anti-reelin (1:500, Chemicon) and rabbit anti-synaptophysin (1:100, Santa Cruz) in TBS with 0.3% Triton-X 100. The tissue was reacted for 48 h at 4 °C with shaking. Following primary antibody incubation, the tissue was blocked in 5% goat serum in TBS with 0.3% Triton-X 100. Primary antibodies were then visualized with fluorophore-conjugated secondary antibodies against the appropriate species (Molecular Probes). Nuclei were counterstained with Hoechst.

For double-labeling of total tau and tau phosphorylated at serine 202, tissue was treated with sodium borohydride as described above, followed by blocking in 5% milk in TBS for 1 h. Sections were then reacted overnight in primary antibodies diluted in 5% milk in TBS; total tau antibodies were used at 1:100 (Dako Cytomation), while the phospho-tau antibody was used at 1:500 (antibody kindly provided by Peter Davies). The following day, sections were washed in TBS containing 0.05% Triton-X 100 and reacted with fluorophore-conjugated secondary antibodies as described above.

Antibody Specificity

Standard immunohistochemical controls included omission of primary antibodies. The specificity of the reelin antibody used in these studies has been determined previously (de Bergeyck et al. 1998). To produce the CP13 antibody against tau phosphorylated at serine 202, mice were immunized with paired helical filament tau purified from AD brain tissue as described by Jicha et al. (1997). The CP13 antibody specifically recognizes the phosphopeptide sequence GYSSPG(phospho-serine 202)PGTPGSRS and does not react with any other phosphoserine site on the tau protein (Jicha et al. 1997). The total tau antibody was raised against the C-terminal part (amino acids 243–441) containing the 4 repeated sequences involved in microtubule binding. The anatomical pattern of staining for total tau was identical to that shown using this antibody in previous studies (Planel et al. 2007), and this antibody has previously been shown to label tau protein independently of its phosphorylation state (Biernat et al. 2002). The synaptophysin antibody detects an epitope corresponding to amino acids 221–313 mapping at the C-terminus of synaptophysin of human origin, with crossreactivity for the synaptophysin protein in rats. The spatial pattern of synaptophysin immunoreactivity was identical to that observed in previous studies (Stranahan et al. 2008), and we tested antibody specificity in tissue from synaptophysin knockout mice (kindly provided by Dr Rudolf Leube). No staining was observed in tissue from synaptophysin knockout mice.

Unbiased Stereology and Anatomical Criteria

For stereological quantification, the optical fractionator method was implemented using the StereoInvestigator morphometry system (MicroBrightField), as described (Rapp et al. 2002). Slides were coded prior to analysis and the code was not broken until the analysis was finished. Neuron counts were derived from bilateral sections through the entire rostrocaudal extent of the entorhinal cortex. The anatomical borders of the lateral and medial entorhinal areas were traced under low-power magnification, and subsequent cell counting was performed within these borders as shown schematically in Figure 2*A* and as described previously for the entorhinal cortex in this study population (Rapp et al. 2002). In detail, the lateral entorhinal cortex was localized anatomically by its position inferior to the rhinal sulcus and by its rostrolateral position relative to the medial entorhinal cortex, as described (Insausti et al. 1997). The lateral entorhinal cortex is bordered rostrally by the perirhinal cortex. Reelin labeling in layer II was restricted to the lateral entorhinal cortex and was not observed in the superficial layers of the perirhinal cortex (Fig. 2*B*,*C*). In this regard, the presence of reelin labeling in layer II is a chemoarchitectonic marker that delineates the lateral entorhinal cortex.

The medial entorhinal cortex abuts the caudal and medial edge of the lateral entorhinal cortex (Fig. 2*A*). The transition from lateral to medial entorhinal cortex was readily apparent based on greater width of the lamina dessicans (layer IV) in the medial relative to the lateral entorhinal cortex. Layer II of the lateral entorhinal cortex exhibits continuous labeling for reelin, relative to the medial entorhinal cortex, consistent with the cellular architectonics in these regions on Nissl-stained preparations (Rapp et al. 2002). Thus, we defined the border between the lateral and medial entorhinal cortices using anatomical criteria with reference to Paxinos and Watson (1998) and cytoarchitectural criteria with reference to the continuity (lateral) or clustering (medial) of layer II neurons. The medial entorhinal cortex is bordered by the parasubiculm on its medial surface, and the transition between the medial entorhinal cortex and the parasubiculum is demarcated by a dramatic increase in the thickness of layer II (Rapp et al. 2002). Cells were viewed through a 40× objective and counted as they first came into focus within each optical disector. Counts derived from these samples were converted to estimates of total labeled cell numbers for each region.

Confocal Microscopy and Typhoon Imaging

Analysis of synaptophysin labeling in the entorhinal cortex was carried out as described in Stranahan et al. (2008). Briefly, images of synaptophysin labeling were captured on a Zeiss LSM 510 Meta confocal microscope. The frame size was 71.43 × 71.43 μm with 512 × 512 pixel density. Ten frames per animal were collected from superficial layers of the lateral and medial entorhinal areas, with sampling spaced evenly throughout the rostrocaudal extent of these regions. Quantitative analysis was carried out using LSM 510 software.

To acquire images of tau and phospho-tau labeling that could be sampled across larger regions of the entorhinal cortex, we used a typhoon fluorescent imaging system (GE Healthcare). For this analysis, the 488 excitation channel was captured at the 520 emission setting with bandpass 40 filtering. The 532 excitation channel was captured at 610 emission with bandpass 30 filtering. For both channels, the photomultiplier tube was set to 500 V. This scanning method has a 10 μm minimum resolution and allowed us to measure immunoreactivity for tau and phospho-tau in the same tissue sections using ImageJ. Grayscale optical density values for phosphorylated tau and total tau were averaged across anatomically matched tissue sections to give a single score for each brain region in each animal.

In Situ Probe Synthesis

Probe templates were synthesized as described in Haberman et al. (2008). Initial primer sequences were as follows: for reelin, left, agtactcagacgtgcagtgg, right, ctcatgaagcaaagtccaa; for DAB1, left, gaacaagccgtgtaccagac, right, agagccaaacacatctgcac. Polymerase chain reaction (PCR) products were verified by restriction endonuclease digestion. Initial PCR products were amplified further with the same PCR primers that had been modified by the addition of T7 or SP6 RNA polymerase-binding sites. PCR products containing T7 and SP6 extensions were purified by SVgel and a PCR cleanup kit (Promega). 35S-uridine triphosphate (UTP)–labeled riboprobe was then generated using the Maxiscript kit (Ambion). The probe was then phenol/choloroform extracted and precipitated in ethanol at –80 °C. The final probe was resuspended in RNase-free water and the specific activity was determined by scintillation counter.

In Situ Hybridization

In situ hybridization was carried out as described by Haberman et al. (2008). All tissue for each individual probe was processed during a single run. Free-floating tissue sections were washed in 0.75% glycine in 0.1 M phosphate buffer 2 times, followed by a single wash in phosphate buffer. After that, sections were reacted in proteinase K buffer containing 1.0 μg/mL proteinase K for 30 min at 37 °C. Sections were then treated with acetic anhydride solution (11.3% triethanolamine, 0.25% acetic anhydride, 0.04 M acetic acid) for 10 min at room temperature. This was followed by two 15-min washes in 2× sodium chloride/citrate buffer (SSC buffer; 20× concentration, 3 M NaCl, 0.3 M sodium citrate). Next, sections were transferred to hybridization buffer containing 20% formamide, 0.4× Denhardt's solution, 4% dextran sulfate, and 1.6× SSC) supplemented with 0.25 mg/mL transfer RNA, 0.33 mg/mL sheared salmon sperm DNA, 100 mM dithiothreitol (DTT), and 1×10^7 cpm/mL 35S-UTP–labeled probe for overnight reaction at 60 °C. The following day, sections were washed at 60 °C in 4× SSC/0.01 M DTT and 2× SSC/50% formamide. They were then incubated with RNase (20 μg/mL) at 37 °C for 30 min. Sections were washed with progressively decreasing concentrations of SSC before mounting on slides.

Densitometry of In Situ Hybridization mRNA Labeling

Slides processed for in situ hybridization were exposed to a phosphoimager screen and quantified by using ImageQuant (GE Healthcare). Digital images were acquired for entorhinal cortical sections from the same levels for all animals. We analyzed (n = 5) sections per animal from lateral entorhinal cortex, with sampling extending from bregma –4.80 to bregma –8.72 (Paxinos and Watson 1998). In the medial entorhinal cortex, we sampled (n = 3) sections per animal from bregma –6.30 to bregma –9.16, as shown in Figure 2*A*. The subregion of interest was outlined by hand by a researcher who was blind to group conditions. Sections were averaged to obtain a single score for each animal.

Statistics

Behavioral data were compared across young and aged rats using repeated-measures analysis of variance (ANOVA) with trial block as a repeated measure and age as a fixed factor, followed by Bonferroni post hoc analysis. Learning indices and physiological data were compared across young, aged-unimpaired, and aged-impaired rats using ANOVA with a planned post hoc comparison. The planned comparison was designed to characterize differences between behaviorally impaired aged rats (AI) and young and aged behaviorally intact rats (Y+AU). Correlations between physiological measures and learning indices among the rats in the aged cohort were made using Pearson's correlation analysis. Our rationale for including both aged-impaired and aged-unimpaired in the correlation analyses is described in detail by Baxter and Gallagher (1996). For all analyses, statistical significance was set at $P < 0.05$.

Results

Aged Rats Exhibit a Range of Cognitive Abilities on a Task that Depends on Medial Temporal Lobe Function

Twenty-four-month-old male Long-Evans rats navigate less effectively to the hidden platform in the Morris water maze, relative to young rats, during training trials (Fig. 1*A*; $F_{1,42}$ = 12.64, $P < 0.0001$). The difference in performance on the first block of training trials represents greater improvement across those initial trials in young rats, as the aged rats performed on par with the young rats during the first trial of maze training (t_{42} = 0.25, P = 0.81). As reported elsewhere, aged rats in this study population exhibit individual differences as assessed using an index score derived from the mean distance from the platform location during probe trials (Fig. 1*B*; Gallagher et al. 1993). While a considerable number of the aged rats were unimpaired with low index scores similar to young adults, others in the aged cohort fell outside the range of young performance. Note that the scores for the young rats, index <240, in this study were in the normative range previously

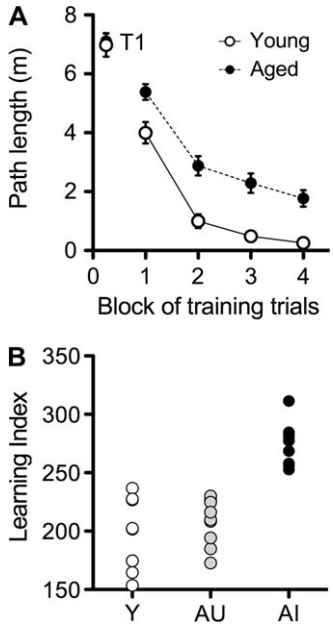

Figure 1. Behavioral characterization on a task that recruits temporal lobe structures identifies a subpopulation of aged rats that are impaired relative to young adults. (*A*) Aged male Long-Evans rats follow a more circuitous path to the hidden platform in the water maze over the course of training. Differences in performance on the first block of trials are not detectable during the first trial (T1). Data points represent the mean of blocks of 5 trials, and error bars depict the standard error of the mean. (*B*), The learning index score, derived from the average distance from the platform location during interpolated probe trials (described in Materials and Methods and in Gallagher et al. 1993), distinguishes between aged-unimpaired (AU) and aged-impaired (AI) rats.

observed with this protocol (Gallagher et al. 1993). Using this index, we characterized the aged rats as either impaired or unimpaired relative to young for immunohistochemical analysis.

Aged-Impaired Rats Have Fewer Reelin Immunoreactive Cells in the Lateral Entorhinal Cortex

The lateral and medial subdivisions of the entorhinal cortex are readily apparent on coronal sections (shown schematically in Fig. 2*A*). Immunoreactivity for reelin delineates the layer II neurons of the entorhinal cortex (Figs 2*B–D* and 3*A*,*B*). Stereological analysis revealed that aged cognitively impaired rats have fewer reelin-positive cells in the lateral entorhinal cortex, relative to young rats and aged rats with preserved cognition (Fig. 3*B*,*C*; $F_{2,26}$ = 4.51, P = 0.022). There was no significant difference in reelin-positive cell numbers in the medial entorhinal cortex ($F_{2,26}$ = 0.001, P = 0.99).

Changes in the number of reelin-immunoreactive cells are unlikely to be attributable to loss of neurons, as previous work in this model (Rapp et al. 2002) and in Fischer rats (Merrill et al. 2001) has shown no change in total neuron number in the lateral entorhinal cortex with age-related cognitive impairment. Taken together with the current report, these observations would indicate a loss of reelin expression in neurons in the lateral entorhinal cortex of aged rats that are cognitively impaired. We also looked at the relationship between reelin-immunoreactive cell counts and behavioral performance among rats in the aged cohort. While spatial memory impairment, indicated by higher index scores, was generally related to reduced reelin immunoreactive neuron numbers in the lateral entorhinal cortex, this trend was not statistically significant (Pearson's r = –0.43, P = 0.075).

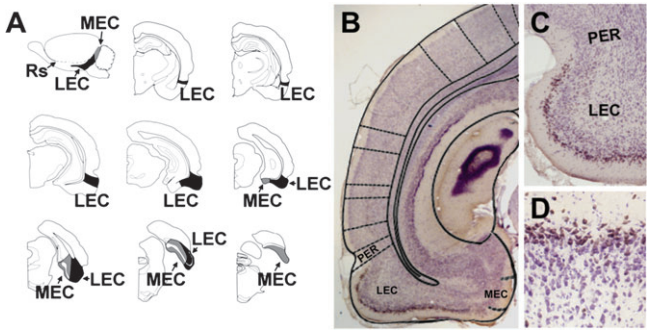

Figure 2. Reelin is a marker expressed by neurons in the superficial layers of the lateral entorhinal cortex. (*A*) Sagittal view of the rat brain, showing the anterior and inferior anatomical position of the lateral entorhinal cortex (LEC) and the posterior situation of the medial entorhinal cortex (MEC). The LEC is visible on coronal sections containing the dorsal hippocampus. As sections become more caudal, the LEC occupies more of the temporal cortex. On caudal sections that do not contain hippocampus, the MEC is visible at the medial edge of the cortex. Eventually, the MEC ascends to encompass the temporal cortical field. Image in (*A*) adapted from Rapp et al. (2002). (*B*) Low-magnification image showing reelin immunoreactivity in the superficial layers of the LEC. The diagram superimposed on the image is from Paxinos and Watson (1998). (*C*) Reelin staining in layer II is confined to the LEC, located inferior to the rhinal sulcus on coronal sections. No reelin staining is detected in layer II of perirhinal cortex (PER) surrounding the superficial portion of the rhinal sulcus. (*D*) Immunoreactivity for reelin among neurons in layer II of the lateral entorhinal cortex.

Reelin mRNA Expression Is Reduced in the Lateral Entorhinal Cortex of Aged-Impaired Rats

In agreement with the observed decrease in reelin-positive cells in lateral entorhinal cortex, a corresponding reduction in reelin mRNA expression was observed in a separate set of aged rats. Behavioral performance for this cohort of aged rats distinguished between aged rats that are cognitively impaired or unimpaired, relative to young rats (Fig. 4*A*). Aged rats that are cognitively impaired exhibit reduced reelin mRNA expression in the lateral entorhinal cortex (Fig. 4*B*,*C*; $F_{2,16}$ = 19.94, P = 0.001) with no change in reelin mRNA expression in the medial entorhinal cortex ($F_{2,12}$ = 1.76, P = 0.21). Reelin mRNA expression again followed an anatomical gradient, such that greater signal was detected in the lateral entorhinal cortex, relative to the medial entorhinal cortex (Fig. 4*C*). There was no effect of aging or cognitive status on mRNA for reelin's intracellular signaling target, "disabled"-1 (Supplementary Fig. 1). No significant

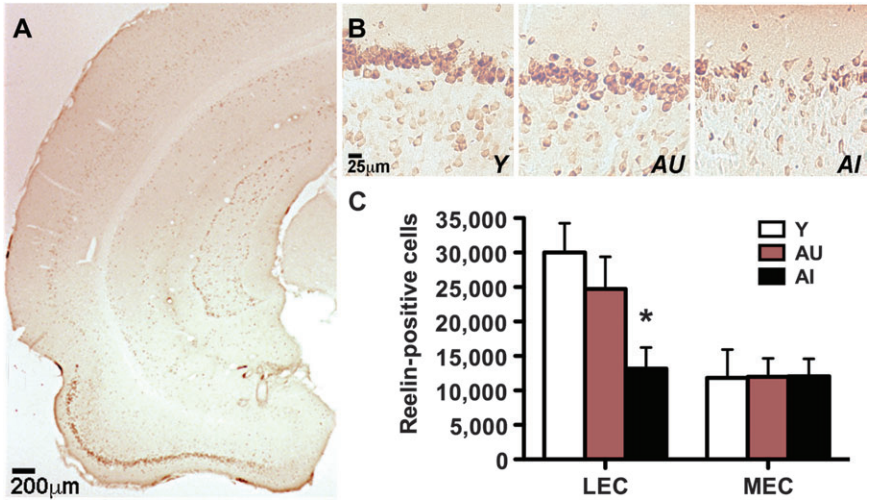

Figure 3. Aged rats that are cognitively impaired have fewer reelin-immunoreactive cells in the lateral entorhinal cortex. (*A*) Representative photomicrograph showing reelin labeling in the entorhinal cortex of a young rat. (*B*) Higher magnification image showing reelin immunoreactivity in layer II of the entorhinal cortex in a representative young rat (Y), a representative aged-unimpaired rat (AU), and a representative aged-impaired rat (AI). (*C*) Aged-impaired rats have significantly fewer reelin-positive cells in the lateral entorhinal cortex (LEC), relative to young rats. No changes were apparent in the medial entorhinal cortex (MEC). Asterisk indicates significance at $P < 0.05$ following one-way ANOVA with planned post hoc comparison between behaviorally impaired rats (AI) and behaviorally intact rats (AU+Y). Error bars represent the standard error of the mean.

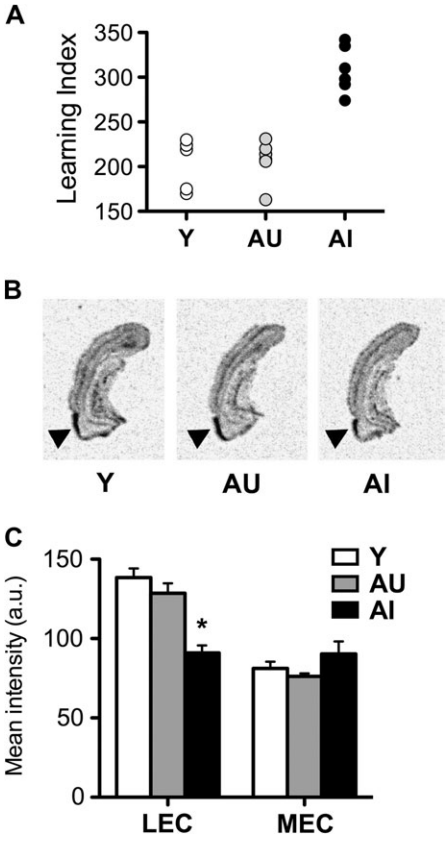

Figure 4. Age-related cognitive impairment is associated with reduced reelin mRNA expression in the lateral entorhinal cortex. (*A*) A subset of aged rats exhibits impaired learning in the water maze. Rats were classified based on a proximity metric, with higher scores indicating poor memory for the platform location (Gallagher et al. 1993). (*B*) Representative images of entorhinal cortical sections visualizing reelin mRNA expression in young (Y), aged-unimpaired (AU), and aged-impaired (AI) rats. (*C*) Aged cognitively impaired rats exhibit reduced reelin mRNA expression in the lateral entorhinal cortex (LEC), with no change in reelin expression in the medial entorhinal cortex (MEC). Asterisk indicates significance at $P < 0.05$ following one-way ANOVA with planned post hoc comparison between behaviorally impaired rats (AI) and behaviorally intact rats (AU+Y). Error bars represent the standard error of the mean.

correlations were found between reelin or DAB1 mRNA expression and the learning index among rats in this cohort of aged subjects.

Alterations in Tau Phosphorylation with Age-Related Cognitive Impairment

Tangles composed of hyperphosphorylated tau form earlier in the lateral entorhinal cortex, relative to the medial entorhinal cortex, during aging and neurodegenerative disease in humans (Arriagada et al. 1992; Braak H and Braak E 1995). While reelin negatively regulates tau phosphorylation (Hiesberger et al. 1999), there are multiple tau kinases and several modulatory factors that could underlie the regional susceptibility of the lateral entorhinal cortex during aging and AD. To evaluate another cellular event known to be a characteristic of the aging lateral entorhinal cortex, we measured phosphorylation of tau at serine 202 using immunohistochemistry.

Aged-impaired rats exhibit increased tau phosphorylation in the lateral entorhinal cortex, relative to young rats (Fig. 5*A*,*B*; $F_{2,26} = 11.03$, $P = 0.004$). Accumulation of phosphorylated tau was also correlated with behavioral performance among aged rats, such that a greater increase in tau phosphorylation was

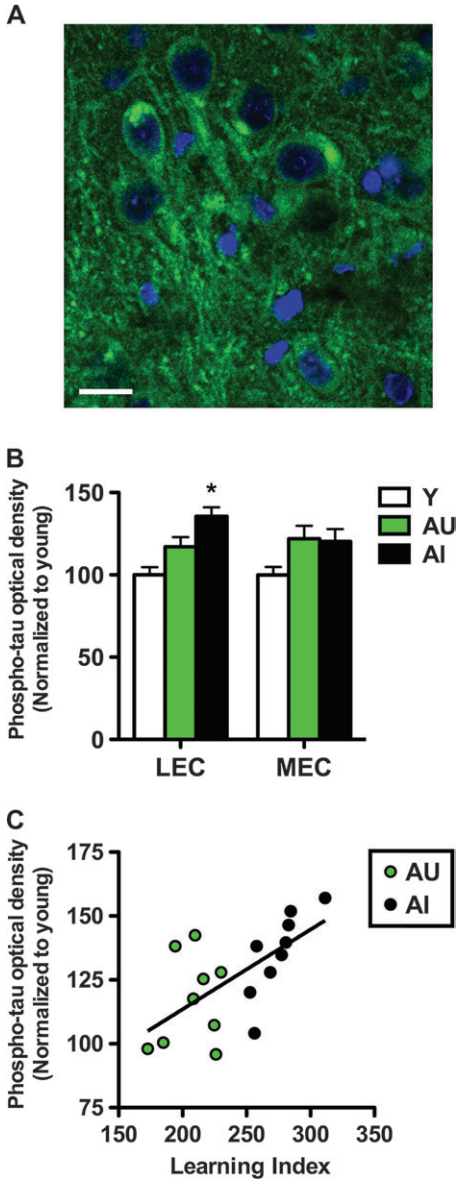

Figure 5. Increased phosphorylated tau immunoreactivity in the lateral entorhinal cortex accompanies reelin depletion in aged-impaired rats. (*A*) Confocal micrograph showing somatodendritic inclusions of phosphorylated tau in the lateral entorhinal cortex of an aged-impaired rat. (*B*) Optical densities for the phosphorylated tau signal on typhoon scanning images. Aged-impaired rats exhibit increased phospho-tau signal in the lateral entorhinal cortex (LEC), with no significant change detected in the medial entorhinal cortex (MEC). Asterisk indicates significance at $P < 0.05$ following one-way ANOVA with planned post hoc comparison between behaviorally impaired rats (AI) and behaviorally intact rats (AU+Y). Error bars represent the standard error of the mean. (*C*), Among the aged rats, levels of phospho-tau immunoreactivity in the lateral entorhinal cortex are correlated with cognitive performance. No such correlation was found in the medial entorhinal cortex. Correlations were determined using Pearson's correlation with $P < 0.05$ as described in Materials and Methods.

associated with worse behavioral performance (Fig. 5*C*; Pearson's $r = 0.64$, $P = 0.004$). By contrast, there was no effect of aging or cognitive status on total tau immunoreactivity in the lateral entorhinal cortex ($F_{2,26} = 0.74$, $P = 0.49$; Supplementary Fig. 2). Insofar, as total tau expression reflects neuronal integrity, the absence of change in total tau immunoreactivity is consistent with other evidence that total neuron number is unchanged in the lateral entorhinal cortex of aged-impaired rats (Merrill et al. 2001; Rapp et al. 2002).

We observed no significant change in total tau expression ($F_{2,26}$ = 1.73, P = 0.20; Supplementary Fig. 2) in the medial entorhinal cortex. There was a strong nonsignificant trend for the main effect of aging, independent of behavioral performance and cognitive status, on tau phosphorylation in medial entorhinal cortex (Fig. 5*B*; $F_{2,26}$ = 3.29, P = 0.055). As expected based on that trend, tau phosphorylation in the medial entorhinal cortex did not correlate with behavioral alterations in the water maze among the aged rats (Pearson's r = 0.26, P = 0.31).

Loss of Reelin Immunoreactivity in the Lateral Entorhinal Cortex Is Accompanied by Local Reductions in Synaptic Marker Expression

While neuron numbers are largely preserved throughout the hippocampal formation and medial temporal cortex in aged rats with cognitive impairment (Rapp and Gallagher 1996; Rapp et al. 2002), a circuit-specific loss of synapses has been found in aged rats with cognitive impairment involving the innervation to the hippocampus originating in layer II entorhinal cortex (Smith et al. 2000). Local intrinsic connections involving layer II collaterals also exist within the entorhinal cortex itself, through a network of ascending fibers traversing superficial layers. (Supplementary Fig. 3, and van Strien et al. 2009). We used synaptophysin immunoreactivity, which labels presynaptic terminals, to provide a preliminary estimate for loss of synaptic integrity that might be associated with intrinsic connections of layer II neurons.

The expression of reelin in neurons in the superficial layers of the entorhinal cortex using immunofluorescence is shown in Figure 6*A*. Fluorescence labeling for synaptophysin is also evident in layer II of the entorhinal cortex, surrounding the dendritic fields of reelin-labeled cells (Fig. 6*A*,*B*). Analysis of this labeling for synaptophysin showed a significant reduction in the lateral entorhinal cortex of aged-impaired rats (Fig. 6*C*; $F_{2,26}$ = 4.59, P = 0.02). In contrast, there was no statistically significant effect of aging or cognitive status on synaptophysin immunoreactivity in the medial subregion ($F_{2,26}$ = 1.30, P = 0.29). These data suggest that inputs to the superficial layers of the lateral entorhinal cortex are diminished, although the source of those inputs, either extrinsic or intrinsic, remains to be determined. However, we did observe that phospho-tau accumulation was inversely correlated with synaptophysin immunoreactivity (Pearson's r = –0.60, P = 0.008; Fig. 6*D*). This is notable because tau phosphorylation has been linked to synaptic loss (Spires-Jones et al. 2009).

Discussion

We have identified a number of changes associated with individual differences in neurocognitive aging in the lateral

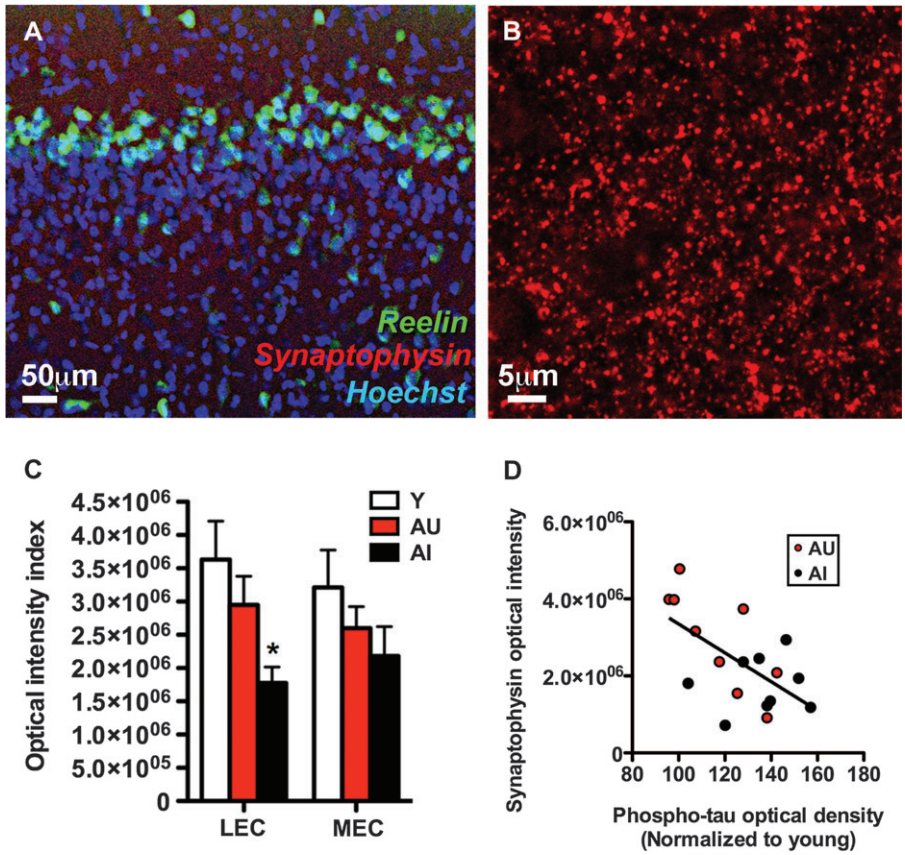

Figure 6. Reductions in synaptophysin labeling occur in concert with loss of reelin expression in the lateral entorhinal cortex of aged-impaired rats. (*A*) Immunoreactivity for the synaptic marker synaptophysin is detectable in the dendritic fields of reelin-immunoreactive cells in the entorhinal cortex. (*B*) Confocal micrograph showing synaptophysin-immunoreactive puncta in the superficial layers of the lateral entorhinal cortex in a young rat. (*C*) Labeling for the synaptic marker synaptophysin is reduced in the lateral entorhinal cortex (LEC) of aged-impaired rats, with no significant alterations detected in the medial entorhinal cortex (MEC). Asterisk indicates significance at $P < 0.05$ following one-way ANOVA with planned post hoc comparison between behaviorally impaired rats (AI) and behaviorally intact rats (AU+Y). Error bars represent the standard error of the mean. (*D*) Synaptophysin optical intensity was inversely correlated with tau phosphorylation in aged rats. Correlations were determined using Pearson's correlation with $P < 0.05$ as described in Materials and Methods.

entorhinal cortex. Reelin expression is reduced at both the protein and mRNA level in aged rats that are cognitively impaired. Changes in reelin expression occurred in the context of increased tau phosphorylation and reduced synaptic marker immunoreactivity. These changes followed a consistent anatomical pattern, such that the lateral entorhinal cortex emerged as a focal region in aged rats with impaired cognitive status.

Alterations in reelin expression, synaptophysin immunoreactivity, and tau phosphorylation occurred in the lateral entorhinal cortex of aged rats with spatial memory impairment. By contrast, aged rats with preserved behavioral performance exhibited few alterations compared with young adults. However, individual differences in this model of cognitive aging are not confined to spatial tasks. Aged rats that are behaviorally impaired in the water maze also exhibit reduced odor recognition memory (Robitsek et al. 2008), a function that involves the lateral entorhinal cortex (Young et al. 1997). In this regard, neurobiological alterations observed in the lateral entorhinal cortex in the current experiments could directly contribute to olfactory recognition deficits reported in aged rodents (LaSarge et al. 2007; Robitsek et al. 2008) and in humans with MCI and AD (Djordjevic et al. 2008). These changes might additionally exert downstream effects on hippocampal networks by disrupting entorhinal connectivity, which would alter the fidelity of information transmitted to the hippocampus.

The functional consequences of reduced reelin expression with age-related cognitive decline have yet to be elucidated, but the findings in the current study point to the lateral entorhinal cortex as a relevant network for such studies. Reelin is transported along perforant path axons and released within the terminal zones of entorhinal layer II afferents (Martínez-Cerdeño et al. 2003). During aging, synaptic plasticity at lateral perforant path synapses in the dentate gyrus is reduced (Froc et al. 2003), but the question of whether changes in reelin expression contribute to synaptic plasticity deficits has not been addressed. Moreover, although there is significant support for a reelinergic contribution to long-term potentiation at Schaffer collateral synapses in CA1 (for review, see Herz and Chen 2006), the association between reelin expression and synaptic plasticity at lateral perforant path synapses has not been characterized.

Reelin regulates neuronal migration during development and synaptic number and function during adulthood (Herz and Chen 2006). Transgenic overexpression of reelin in neurons during adulthood increases the number of synapses in regions of the hippocampus that receive input from layer II neurons (Pujadas et al. 2010). In contrast, heterozygous reeler mice, which exhibit a nearly 50% reduction in reelin levels, have fewer hippocampal synapses (Niu et al. 2008). Functionally, reelin enhances long-term potentiation and protects against deficits induced by application of β-amyloid (Durakoglugil et al. 2009). This opens the possibility that reelin produced by the entorhinal cortex could confer neuroprotection on target cells in the hippocampus, which would be compromised with loss of reelin expression during age-related cognitive decline.

The observation that AD mice have fewer reelin immunoreactive principal neurons in the entorhinal cortex (Chin et al. 2007) without overt loss of entorhinal neurons (Irizarry et al. 1997) suggests that reduced reelin expression may contribute to early synaptic alterations in AD. While previous studies examining differences in reelin expression in AD mouse models did not differentiate between the medial and lateral entorhinal cortices, the topography of changes in the terminal zones innervated by entorhinal subdivisions suggests particular lateral entorhinal sensitivity. The outer molecular layer, which receives input from the lateral entorhinal cortex, shows the earliest synaptic atrophy (Dong et al. 2007) and accumulation of amyloid deposits (Reilly et al. 2003). This synaptic zone is similarly subject to loss of connectivity in the same population of aged rats used in the current study (Smith et al. 2000). Here, we show that reduced reelin expression is also seen in the context of changes in synaptic marker expression in the lateral entorhinal cortex during normal age-associated cognitive decline.

Reduced reelin expression occurred in concert with increased tau phosphorylation and reduced immunoreactivity for the synaptic marker synaptophysin. The lateral entorhinal cortex exhibited specific vulnerability to these molecular alterations during cognitive impairment in aging. A lateral to medial entorhinal topography has long been recognized in human aging, as tangles initially appear in the transentorhinal cortex with progressive involvement of entorhinal layer II neurons along a lateral to medial gradient (Braak stages 1–2) (Braak H and Braak E 1995). Although neurofibrillary tangles do not occur in aged rats, increased phosphorylation of tau emerges in the lateral entorhinal region in older animals exhibiting cognitive decline. The current study is, to the best of our knowledge, the first report of increased tau phosphorylation in the aged rat. A prior report described a redistribution of phospho-tau from neuronal processes to the soma in aged rats (Niewiadomska et al. 2005) but did not quantify phosphorylated tau immunoreactivity in relation to cognitive status. Mice, in contrast with rats, do not display phosphorylated tau accumulation with aging unless expression of wild-type human tau is present under a transgene (Kimura et al. 2007). This distinction may be attributable to differential expression of tau isoforms between the rat and mouse (Takuma et al. 2003), with the rat more closely resembling human tau isoforms.

The current findings have revealed a particular susceptibility of the lateral entorhinal cortex in age-related cognitive impairment. While these observations are best viewed at present as correlates of behavior rather than mechanisms, we have begun to establish a framework for understanding lateral entorhinal vulnerability in neurocognitive aging. In our model, cognitive impairment with aging is associated with reduced reelin expression, increased tau phosphorylation, and synaptic loss in the lateral entorhinal cortex. Future studies will address the mechanistic interrelationships among these changes and their impact on cognitive function.

Supplementary Material

Supplementary material can be found at: http://www.cercor.oxfordjournals.org/.

Funding

National Institute on Aging at the National Institutes of Health (T32 AG027668-02 to A.M.S.); Ford Foundation/National Research Council Fellowship to A.M.S.; National Institute on Aging at the National Institutes of Health (5P01AG009973-17 to M.G.)

Notes

We are grateful to Dr Rebecca Burwell for kindly letting us use her StereoInvestigator system, to Dr Peter Davies of Yeshiva University for

the phosphorylated tau antibody, and to Dr Rudolf Leube of University of Mainz for the synaptophysin knockout mouse tissue. *Conflict of Interest*: M.G. is the founder of AgeneBio Incorporated, a biotechnology company that is dedicated to commercializing therapies to treat cognitive impairment in aging and she has a financial interest in the company. Two of the authors (R.P.H. and M.G.) are inventors on Johns Hopkins University intellectual property with patents pending under option to license to AgeneBio. Dr Gallagher serves as a member of the Board of Scientific Counselors to the National Institute on Aging and is also a member of the Scientific Advisory Board of the Stanley Center at the Broad Institute.

References

Arriagada PV, Marzloff K, Hyman BT. 1992. Distribution of Alzheimer-type pathologic changes in nondemented elderly individuals matches the pattern in Alzheimer's disease. Neurology. 42:1681–1688.

Baxter MG, Gallagher M. 1996. Neurobiological substrates of behavioral decline: models and data analytic strategies for individual differences in aging. Neurobiol Aging. 17:491–495.

Biernat J, Wu YZ, Timm T, Zheng-Fischhöfer Q, Mandelkow E, Meijer L, Mandelkow EM. 2002. Protein kinase MARK/PAR-1 is required for neurite outgrowth and establishment of neuronal polarity. Mol Biol Cell. 13:4013–4028.

Boric K, Muñoz P, Gallagher M, Kirkwood A. 2008. Potential adaptive function for altered long-term potentiation mechanisms in aging hippocampus. J Neurosci. 28:8034–8039.

Braak H, Braak E. 1995. Staging of Alzheimer's disease-related neurofibrillary changes. Neurobiol Aging. 16:271–278.

Chin J, Massaro CM, Palop JJ, Thwin MT, Yu GQ, Bien-Ly N, Bender A, Mucke L. 2007. Reelin depletion in the entorhinal cortex of human amyloid precursor protein transgenic mice and humans with Alzheimer's disease. J Neurosci. 27:2727–2733.

de Bergeyck V, Naerhuyzen B, Goffinet AM, Lambert de Rouvroit C. 1998. A panel of monoclonal antibodies against reelin, the extracellular matrix protein defective in reeler mutant mice. J Neurosci Methods. 82(1):17–24.

Djordjevic J, Jones-Gotman M, De Sousa K, Chertkow H. 2008. Olfaction in patients with mild cognitive impairment and Alzheimer's disease. Neurobiol Aging. 29:693–706.

Dong H, Martin MV, Chambers S, Csernansky JG. 2007. Spatial relationship between synapse loss and beta-amyloid deposition in Tg2576 mice. J Comp Neurol. 500:311–321.

Durakoglugil MS, Chen Y, White CL, Kavalali ET, Herz J. 2009. Reelin signaling antagonizes beta-amyloid at the synapse. Proc Natl Acad Sci U S A. 106:15938–15943.

Froc DJ, Eadie B, Li AM, Wodtke K, Tse M, Christie BR. 2003. Reduced synaptic plasticity in the lateral perforant path input to the dentate gyrus of aged C57BL/6 mice. J Neurophysiol. 90(1):32–38.

Gallagher M, Burwell R, Burchinal M. 1993. Severity of spatial learning impairment in aging: development of a learning index for performance in the Morris water maze. Behav Neurosci. 107:618–626.

Gallagher M, Rapp PR. 1997. The use of animal models to study the effects of aging on cognition. Annu Rev Psychol. 48:339–370.

Geinisman Y, Bondareff W, Dodge JT. 1978. Dendritic atrophy in the dentate gyrus of the senescent rat. Am J Anat. 152:321–329.

Gómez-Isla T, Price JL, McKeel DW Jr, Morris JC, Growdon JH, Hyman BT. 1996. Profound loss of layer II entorhinal cortex neurons occurs in very mild Alzheimer's disease. J Neurosci. 16:4491–4500.

Haberman RP, Lee HJ, Colantuoni C, Koh MT, Gallagher M. 2008. Rapid encoding of new information alters the profile of plasticity-related mRNA transcripts in the hippocampal CA3 region. Proc Natl Acad Sci U S A. 105:10601–10606.

Herz J, Chen Y. 2006. Reelin, lipoprotein receptors and synaptic plasticity. Nat Rev Neurosci. 7:850–859.

Hiesberger T, Trommsdorff M, Howell BW, Goffinet A, Mumby MC, Cooper JA, Herz J. 1999. Direct binding of Reelin to VLDL receptor and ApoE receptor 2 induces tyrosine phosphorylation of disabled-1 and modulates tau phosphorylation. Neuron. 24:481–489.

Hoe HS, Lee KJ, Carney RS, Lee J, Markova A, Lee JY, Howell BW, Hyman BT, Pak DT, Bu G, et al. 2009. Interaction of reelin with amyloid precursor protein promotes neurite outgrowth. J Neurosci. 29:7459–7473.

Insausti R, Herrero MT, Witter MP. 1997. Entorhinal cortex of the rat: cytoarchitectonic subdivisions and the origin and distribution of cortical efferents. Hippocampus. 7:146–183.

Irizarry MC, Soriano F, McNamara M, Page KJ, Schenk D, Games D, Hyman BT. 1997. Abeta deposition is associated with neuropil changes, but not with overt neuronal loss in the human amyloid precursor protein V717F (PDAPP) transgenic mouse. J Neurosci. 17:7053–7059.

Jicha GA, Bowser R, Kazam IG, Davies P. 1997. Alz-50 and MC-1, a new monoclonal antibody raised to paired helical filaments, recognize conformational epitopes on recombinant tau. J Neurosci Res. 48:128–132.

Kimura T, Yamashita S, Fukuda T, Park JM, Murayama M, Mizoroki T, Yoshiike Y, Sahara N, Takashima A. 2007. Hyperphosphorylated tau in parahippocampal cortex impairs place learning in aged mice expressing wild-type human tau. EMBO J. 26:5143–5152.

LaSarge CL, Montgomery KS, Tucker C, Slaton GS, Griffith WH, Setlow B, Bizon JL. 2007. Deficits across multiple cognitive domains in a subset of aged Fischer 344 rats. Neurobiol Aging. 28:928–936.

Martínez-Cerdeño V, Galazo MJ, Clascá F. 2003. Reelin-immunoreactive neurons, axons, and neuropil in the adult ferret brain: evidence for axonal secretion of reelin in long axonal pathways. J Comp Neurol. 463:92–116.

Merrill DA, Chiba AA, Tuszynski MH. 2001. Conservation of neuronal number and size in the entorhinal cortex of behaviorally characterized aged rats. J Comp Neurol. 438:445–456.

Niewiadomska G, Baksalerska-Pazera M, Riedel G. 2005. Altered cellular distribution of phospho-tau proteins coincides with impaired retrograde axonal transport in neurons of aged rats. Ann N Y Acad Sci. 1048:287–295.

Niu S, Yabut O, D'Arcangelo G. 2008. The Reelin signaling pathway promotes dendritic spine development in hippocampal neurons. J Neurosci. 28:10339–10348.

Paxinos G, Watson C. 1998. The rat brain in stereotaxic coordinates. San Diego (CA): Academic Press, Inc.

Planel E, Richter KE, Nolan CE, Finley JE, Liu L, Wen Y, Krishnamurthy P, Herman M, Wang L, Schachter JB, et al. 2007. Anesthesia leads to tau hyperphosphorylation through inhibition of phosphatase activity by hypothermia. J Neurosci. 27:3090–3097.

Pujadas L, Gruart A, Bosch C, Delgado L, Teixeira CM, Rossi D, de Lecea L, Martínez A, Delgado-García JM, Soriano E. 2010. Reelin regulates postnatal neurogenesis and enhances spine hypertrophy and long-term potentiation. J Neurosci. 30:4636–4649.

Ramos-Moreno T, Galazo MJ, Porrero C, Martínez-Cerdeño V, Clascá F. 2006. Extracellular matrix molecules and synaptic plasticity: immunomapping of intracellular and secreted Reelin in the adult rat brain. Eur J Neurosci. 23:401–422.

Rapp PR, Deroche PS, Mao Y, Burwell RD. 2002. Neuron number in the parahippocampal region is preserved in aged rats with spatial learning deficits. Cereb Cortex. 12:1171–1179.

Rapp PR, Gallagher M. 1996. Preserved neuron number in the hippocampus of aged rats with spatial learning deficits. Proc Natl Acad Sci U S A. 93:9926–9930.

Reilly JF, Games D, Rydel RE, Freedman S, Schenk D, Young WG, Morrison JH, Bloom FE. 2003. Amyloid deposition in the hippocampus and entorhinal cortex: quantitative analysis of a transgenic mouse model. Proc Natl Acad Sci U S A. 100:4837–4842.

Robitsek RJ, Fortin NJ, Koh MT, Gallagher M, Eichenbaum H. 2008. Cognitive aging: a common decline of episodic recollection and spatial memory in rats. J Neurosci. 28:8945–8954.

Scheff SW, Price DA, Schmitt FA, Mufson EJ. 2006. Hippocampal synaptic loss in early Alzheimer's disease and mild cognitive impairment. Neurobiol Aging. 27:1372–1384.

Smith TD, Adams MM, Gallagher M, Morrison JH, Rapp PR. 2000. Circuit-specific alterations in hippocampal synaptophysin immunoreactivity predict spatial learning impairment in aged rats. J Neurosci. 20:6587–6593.

Spires-Jones TL, Stoothoff WH, de Calignon A, Jones PB, Hyman BT. 2009. Tau pathophysiology in neurodegeneration: a tangled issue. Trends Neurosci. 32:150–159.

Stranahan AM, Arumugam TV, Cutler RG, Lee K, Egan JM, Mattson MP. 2008. Diabetes impairs hippocampal function through glucocorticoid-mediated effects on new and mature neurons. Nat Neurosci. 11:309–317.

Takuma H, Arawaka S, Mori H. 2003. Isoforms changes of tau protein during development in various species. Brain Res Dev Brain Res. 142:121–127.

van Strien NM, Cappaert NL, Witter MP. 2009. The anatomy of memory: an interactive overview of the parahippocampal-hippocampal network. Nat Rev Neurosci. 10:272–282.

Wilson IA, Gallagher M, Eichenbaum H, Tanila H. 2006. Neurocognitive aging: prior memories hinder new hippocampal encoding. Trends Neurosci. 29:662–670.

Young BJ, Otto T, Fox GD, Eichenbaum H. 1997. Memory representation within the parahippocampal region. J Neurosci. 17:5183–5195.